

Endocrine tumor imaging

Somjai Wangsuphachart*

Kanaungnit Kingpetch*

Wangsuphachart S, Kingpetch K. Endocrine tumor imaging. Chula Med J 2001 Sep; 45(9): 741 - 54

In the present, evaluation of patients with endocrine tumor by radiological imaging is highly beneficial. Clinician can use advanced radiological imaging modalities to diagnose patients with symptoms related to various endocrine diseases. For example, magnetic resonance imaging (MRI) can detect tiny pituitary tumor. Likewise, ultrasonography (US) can diagnose thyroid nodule in patient with suspected having an early thyroid carcinoma. Pre-operative localization of parathyroid adenoma by radionuclide imaging (^{99m}Tc - MIBI Parathyroid scintigraphy) can effectively determine location of tumor especially with post-parathyroidectomy patient. Computed tomography (CT) is another excellent alternative modality for diagnosis of adrenal lesion. However, plain radiograph is still useful for screening musculoskeletal system in some disease eg. acromegaly, hyperparathyroidism. Therefore, it is very crucial for clinician to know and understand how to select appropriate imaging modality of choice for further proper management.

Key word : Endocrine tumor imaging.

Reprint request : Wangsuphachart S, Department of Radiology, Faculty of Medicine,
Chulalongkorn University, Bangkok 10330, Thailand.

Received for publication. May 10,2001.

สมใจ หวังศุภชาติ, คณิงนิจ กิ่งเพชร. การตรวจวินิจฉัยโรคเนื้องอกของต่อมไร้ท่อทางรังสีวิทยา.
จุฬาลงกรณ์เวชสาร 2544 ก.ย; 45(9): 741 - 54

การตรวจวินิจฉัยโรคเนื้องอกของต่อมไร้ท่อทางรังสีวิทยานับว่ามีความสำคัญมาก เนื่องจากในปัจจุบันความก้าวหน้าทางเทคโนโลยีของการวินิจฉัยด้วยภาพ และการตรวจทางรังสีวิทยา ได้ถูกพัฒนาไปอย่างรวดเร็ว ทำให้สามารถวินิจฉัยโรคได้ดีกว่าในอดีตมาก อาทิเช่น การตรวจด้วยคลื่นสะท้อนในสนามแม่เหล็ก (MRI) สามารถช่วยในการวินิจฉัยโรคเนื้องอกของต่อมได้สมอง ได้ตั้งแต่ก้อนยังมีขนาดเล็กและไม่มีอาการ การตรวจด้วยคลื่นเสียงความถี่สูง (US) สามารถวินิจฉัย ก้อนในต่อมธัยรอยด์ในผู้ป่วยที่มีอาการนำสงสัยว่าอาจจะเป็นมะเร็งของต่อมธัยรอยด์แต่ยังคลำก้อนไม่ได้ การตรวจหาตำแหน่งเนื้องอกของต่อมพาราธัยรอยด์ด้วยวิธีทางเวชศาสตร์นิวเคลียร์ สามารถช่วยบ่งบอกตำแหน่งของเนื้องอกได้ดี โดยเฉพาะในผู้ป่วยที่เคยผ่าตัดต่อมพาราธัยรอยด์มาแล้ว การวินิจฉัยโรคของต่อมหมวกไตด้วยเอกซเรย์คอมพิวเตอร์ (CT SCAN) นับเป็นอีกทางเลือกหนึ่งในการวินิจฉัยโรค อย่างไรก็ตามในบางครั้งภาพจากการวินิจฉัยด้วยเอกซเรย์ธรรมดา (plain radiograph) ก็ยังมีประโยชน์ในการวินิจฉัยโรคบางชนิด เช่นผู้ป่วย acromegaly, hyperparathyroidism ซึ่งจะมีการเปลี่ยนแปลงของกระดูกให้เห็นได้ ดังนั้นแพทย์ผู้รักษาจึงต้องมีความรู้และความเข้าใจในการเลือกตรวจวินิจฉัยทางรังสีวิทยาอย่างเหมาะสม เพื่อประโยชน์สูงสุดในการรักษาผู้ป่วย

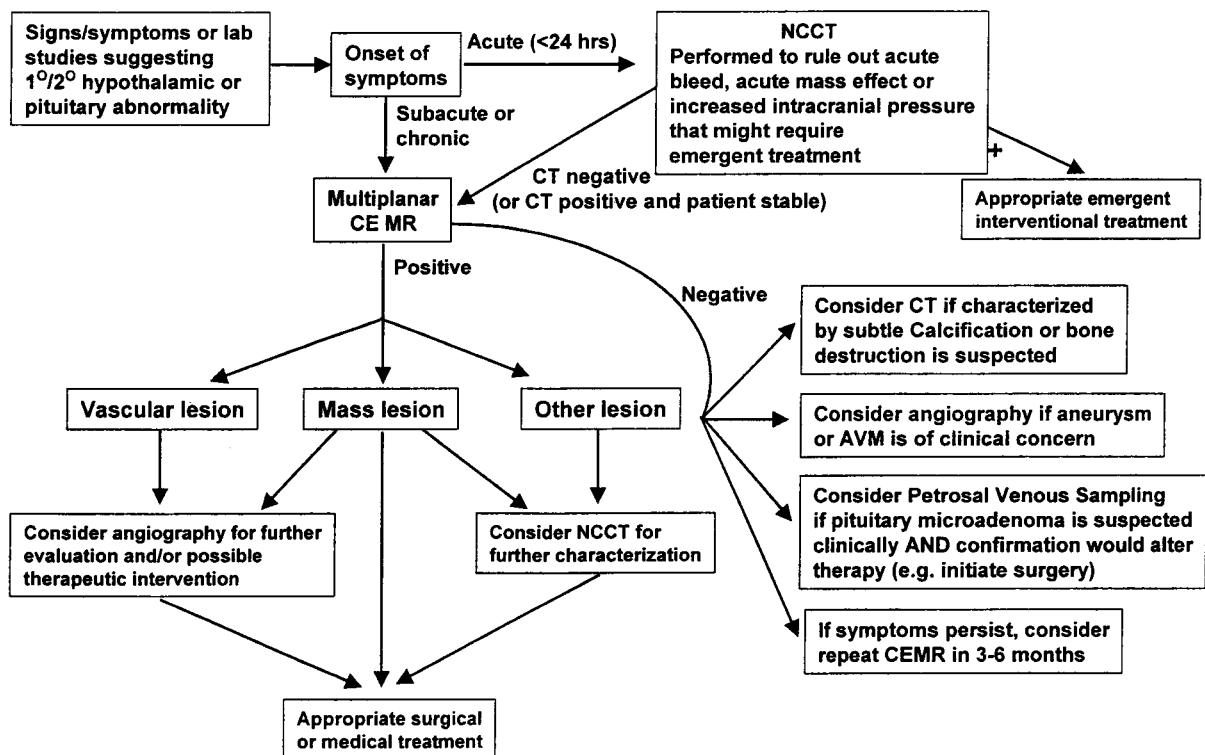
Evaluation of patients with tumor-producing clinically endocrine abnormality is crucial because even a small endocrine tumor can produce high hormonal level which causes severe symptom and sign. Combination of accurate hormonal study and the appropriate imaging of the related endocrine organ lead to the proper management planning and treatment for those patients.

Up to date, high technological imaging modalities such as Magnetic Resonance Imaging (MRI), Computed Tomography (CT), Ultrasonography

(US), Single Proton Emission Computed Tomography (SPECT), venous blood sampling for hormone radioimmunoassay have played important roles in localized endocrine tumor. However, plain radiograph is still useful for musculoskeletal screening in some entities, e.g., acromegaly, hyperparathyroidism.

This article will stress on selection guideline of imaging modalities and tumor localization for common endocrine diseases in six organs i.e., pituitary gland and hypothalamus, pineal gland, thyroid gland, parathyroid glands, adrenal glands and pancreas.

Algorithm 1.



Imaging work up of suspected pituitary or hypothalamic lesion. NCCT = non-contrast CT scan; CEMR = contrast-enhanced MR scan. Other lesion = a lesion which could not be classified by CEMR as vascular or mass lesion

1. Pituitary gland, hypothalamus and parasellar region.

Any imaging abnormality of pituitary gland, hypothalamus or parasellar region must be correlated with endocrine symptoms, signs and hormonal level or electrolyte profiles. MRI is the modality of choice replacing CT scan in detecting abnormality of this region because of its ability to produce multiplanar imagings, lack of ionizing radiation, artifact from adjacent bony ridge and risk avoidance from contrast medium administration. However, additional plain CT is still helpful in detecting abnormal calcification or acute tumoral hemorrhage. The guideline of imaging diagnosis in patients with suspected pituitary or hypothalamic tumor is shown in Algorithm 1.⁽¹⁾

Technique and sequence of MRI protocol include thin slices of both pre and post Gadolinium-DTPA (Gd-DTPA) which is a paramagnetic T1-shortening contrast agent with fat saturation technique in both coronal and sagittal planes.

Normal MRI anatomy in sagittal plane (Figure 1), pituitary gland is well demonstrated in the pituitary fossa above the pneumatized sphenoid sinus. Clivus usually shows bright signal intensity (SI) on T1 weighted image (T1WI) indicating fat marrow. In addition, curving dark SI of lamina dura or cortical bone of the sellar floor is seen. Infundibulum and pituitary stalk extend from hypothalamus downward through diaphragma sella to the junction of anterior and posterior lobe of the pituitary gland. The anterior lobe is isointensity to pons on T1WI and has homogeneous enhancement post Gd-DTPA because there is no blood brain barrier at the gland. Tiny heterogeneity can be seen due to degree of cell packing, granularity, and vascularity of the gland

tissue. The posterior lobe of 52 % of normal population show bright SI on T1WI and the percentage will decrease when patients get older. This bright SI has been claimed to represent fat-laden pituicytes,⁽²⁾ however, there is also a research supporting the presence of axons which contained antidiuretic hormone (ADH) neurosecretory granules.⁽³⁾ The SI of the pituitary gland in both lobes is usually brighter in children comparing to the adults.

The superior border of the gland in coronal plane is usually straight or mild concave with small convex bumping at the midline stalk insertion. Mild convex superior border can be found in female teenagers. The average height of the gland is 5.4 - 5.7 mm. Parasellar structures include cavernous sinuses, internal carotid arteries, cranial nerves III, IV, VI and V2 located superoinferiorly in coronal plane.

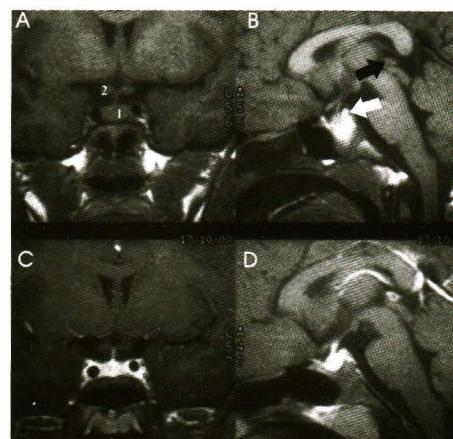


Figure 1. Normal MRI of sellar turcica region

A. coronal view and B. sagittal view show pituitary gland (1) optic chiasm (2) and pineal gland (black arrow) . Anterior lobe and posterior lobe of pituitary gland reveal isointensity and hyperintensity (white arrow) respectively. C. contrast enhanced coronal view (T1WI) and D. contrast-enhanced sagittal view (T1WI) show homogenous enhancement of pituitary gland and pituitary stalk.

Microadenoma is a tumor with its size less than 10 mm. MRI of microadenoma in coronal view (T1WI), immediately after Gd-DTPA administration, will enhance sensitivity of MRI in detecting pituitary microadenoma because the normal gland tissue will enhance more rapidly than the tumor which shows focal hypoSI. (Figure 2) Associated abnormal findings include increased height and convexity of the gland, asymmetry of the sellar floor and deviation of pituitary stalk to contralateral side of the lesion. In case of patients who are clinically suggesting microadenoma but MRI shows normal or inconclusive finding, surgical intervention is needed, inferior petrosal sinus venous sampling is needed for surgical planning by percutaneous transfemoral vein approach and bilateral inferior petrosal sinus catheterization (Figure 3). Venous blood samplings for hormone assay are drawn simultaneously at bilateral inferior petrosal sinuses and peripheral vein to localize the site of the lesion .

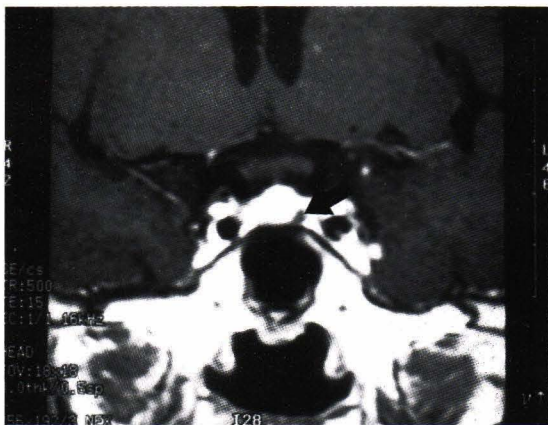


Figure 2. Contrast-enhanced coronal MRI of a 12-year old girl with Cushing's syndrome shows microadenoma (black arrow) on the left side of pituitary gland. (Note : the shape of upper part of pituitary gland in female adolescent may be convex).

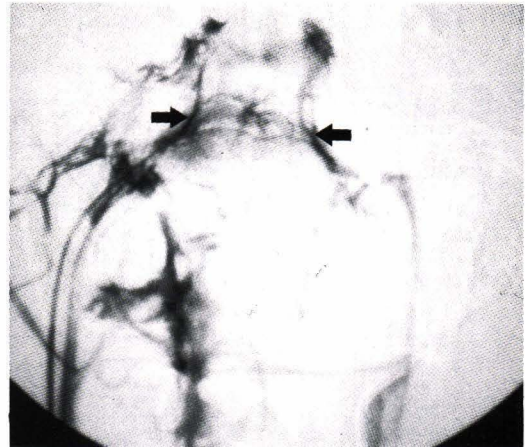


Figure 3. Venous DSA study of base of skull shows bilateral inferior petrosal sinuses (arrows) where venous blood sampling was performed. Serum ACTH of the patient in the figure 2. is
left inferior petrosal sinus = 80.3 pg/ml
(normal =10-16)
right inferior petrosal sinus = 23.8 pg/ml
left anti-brachial vein = 18.3 pg/ml

Macroadenoma is a tumor with its diameter larger than 10 mm. MRI shows isoSI to the gland or relatively slight hypointensity on T1WI because of cystic degeneration. HyperSI due to subacute hemorrhage may be found in 20 - 30%.⁽⁴⁾ MRI cannot differentiate SI between secretory and non-secretory macroadenoma. Macroadenoma with other findings such as thick calvarium and hyperpneumatized paranasal sinuses will confirm the imaging diagnosis of acromegaly. (Figure 4)

Imaging changes after surgical or medical treatment.

Prolactin – secretory microadenoma and small microadenoma are usually treated by ergot derivative e.g. bromocriptine. Forty five percent of the patients who were treated by bromocriptine show intratumoral

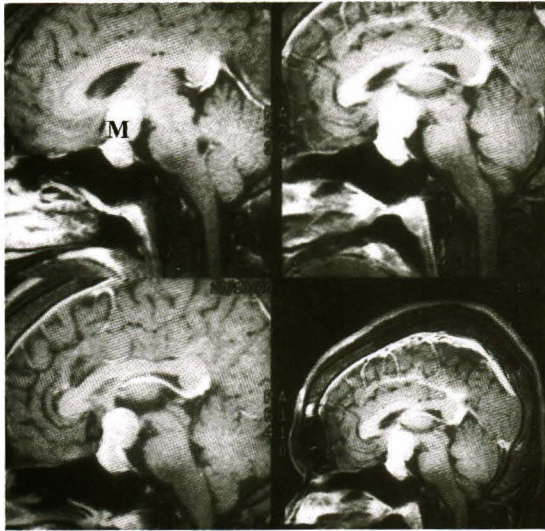


Figure 4. MRI of secretory adenoma shows tumor at pituitary gland (M) with thick calvarium and hyperpneumatized paranasal sinuses which confirm diagnosis of acromegaly.

hemorrhage (bright SI). However, there is also a report showing that 13 % of non-treated patients show intratumoral hemorrhage⁽⁵⁾

Fascia and fat will be found packing in the sphenoid sinus and tumor bed post transphenoidal hypophysectomy. In general, residual/recurrent tumor, residual pituitary glandular tissue, and post surgical scar cannot be exclusively differentiated. Therefore, baseline MRI with follow-up combination of imaging and hormonal level is essential.

2. Pineal gland

Pineal gland is located midline between superior colliculi of midbrain, inferior to the splenium of corpus callosum and posteromedial to the posterior thalami. Before 1980, pineal gland was believed to be a non-functioning gland. Currently, it is supported that the gland produces melatonin related to sleep control and emotional changes.⁽⁶⁾ Pineal tumor usually has nonspecific presenting symptom of increased intracranial pressure because of mass effect on the

cerebral aqueduct resulting to hydrocephalus. Specific less commonly presenting symptoms are parinaud's syndrome, hypothalamic syndrome such as diabetic insipidus, precocious puberty and neuroendocrine syndrome e.g. functional germ cell tumors.

Common mass lesions of pineal gland are categorized in Table 1.

Table 1. Common mass lesions of pineal gland.

Neoplasm	: Teratoma
	: Germinoma
	: Pineal cell tumors
	: pineocytoma
	: pineoblastoma
	: Glioma
	: Metastases
	: Lymphoma / leukemia
	: Meningioma
	Vascular lesions
Granulomatous Lesions	: TB
	: sarcoidosis
Cysts	: Arachnoid
	: Dermoid
	: Epidermoid

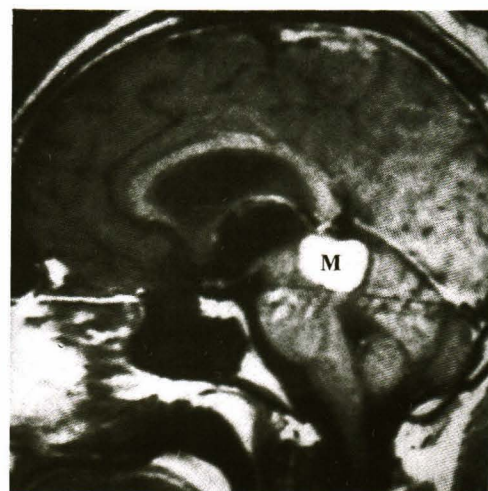


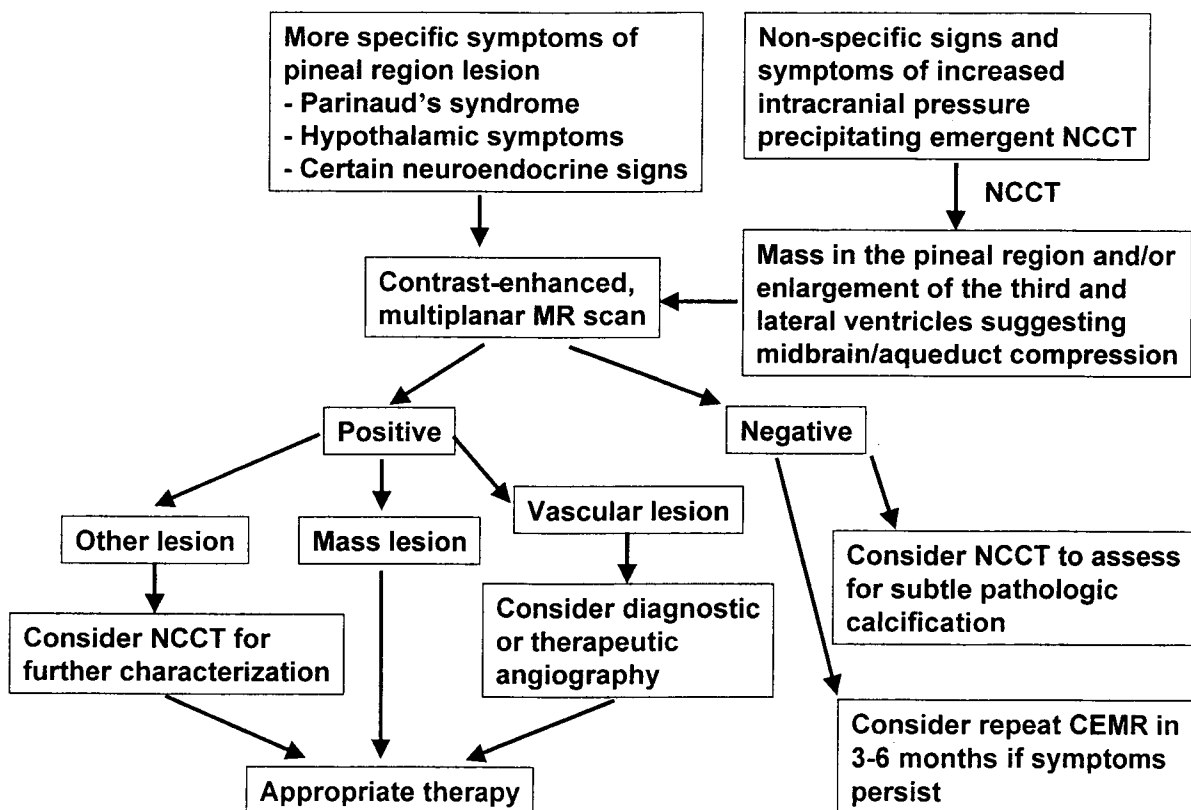
Figure 5. Contrast – enhanced sagittal MRI shows homogeneous well-circumscribed germinoma (M) at pineal gland with cerebral aqueductal obstruction.

MRI is the best modality in demonstrating pineal lesion especially the sagittal plane. The objectives of the investigation not only show location of the pineal gland, relation of the mass, brainstem and adjacent structures but also demonstrate the degree of the cerebral aqueductal obstruction. (Figure 5) The guidelines of imaging diagnosis for patients suspected having pineal lesion are shown in Algorithm 2.

3. Thyroid gland

Thyroid gland is located at anterior aspect of trachea consisting of 2 lobes connected anteriorly by isthmus. Sternocleidomastoid muscles are anteriorly and common carotid arteries are laterally. Ultrasonography (US) is the initial imaging modality for screening of thyroid malignancy. Normal and abnormal ultrasonographic thyroid imagings are shown in Figure 6A and 6B respectively.

Algorithm 2.



Imaging work up of suspected pineal region lesion. NCCT = non-contrast CT scan; CEMR = contrast-enhanced MR scan. Other lesion = a lesion which could not be classified by CEMR as vascular or mass lesion

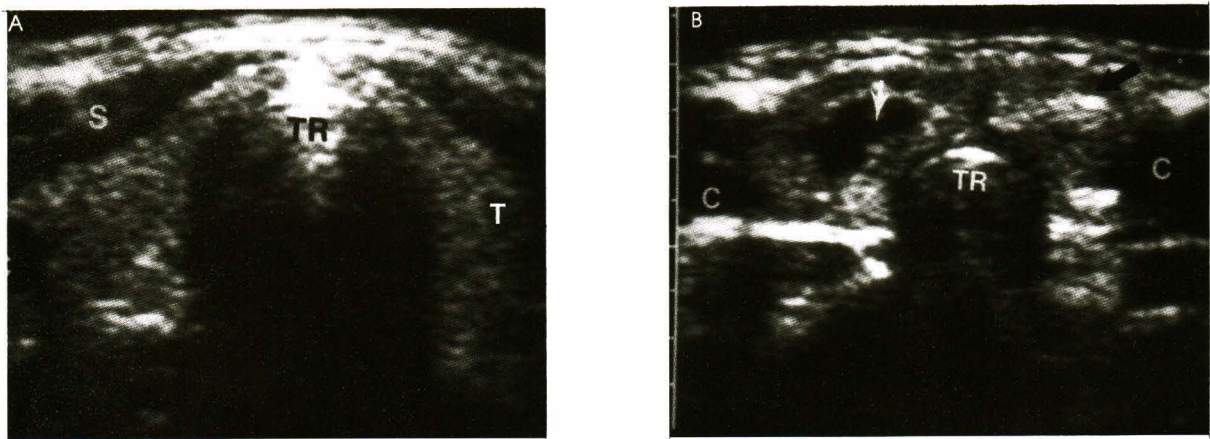


Figure 6. A. Normal ultrasonography of thyroid gland(T), horizontal section reveals higher echogenicity than sternocleidomastoid muscle (S).

B. Ultrasonography of multinodular goiter, horizontal section reveals inhomogeneous echogenicity of thyroid gland due to cystic (white arrow) and solid (black arrow) nodules.

TR = trachea, C = common carotid artery

The objectives of thyroid gland investigations and diagnostic imaging modality of choice for each objective are summarized in Table 2 and the examples

of scintigraphic imagings such as cold nodule and toxic adenoma are shown in Figure 7A and 7B respectively.

Table 2. Radiological diagnostic imaging modalities for thyroid diseases.

Objective	Modality diagnosis
1. To look for abnormal non-palpable thyroid nodule in patient with suspected thyroid carcinoma	US
2. To distinguish abnormal palpable thyroid nodule (solid nodule, cystic nodule, calcified or cystic degenerative nodule)	US
3. To determine function of abnormal thyroid nodule (hyperfunctioning, hypofunctioning or nonfunctioning thyroid nodule)	Thyroid scintigraphy
4. To diagnose cervical lymph node metastasis in patient with thyroid carcinoma	CT or MRI
5. To look for extrathyroidal extension (eg. trachea, carotid artery) in patient with thyroid carcinoma	CT or MRI
6. To determine vascularity of tumor mass prior to biopsy or after suppressive therapy	Color flow Doppler imaging
7. To look for local recurrence or persistent residual tissue after treatment in patient with differentiated thyroid carcinoma	Total body scan (^{131}I) or CT or MRI

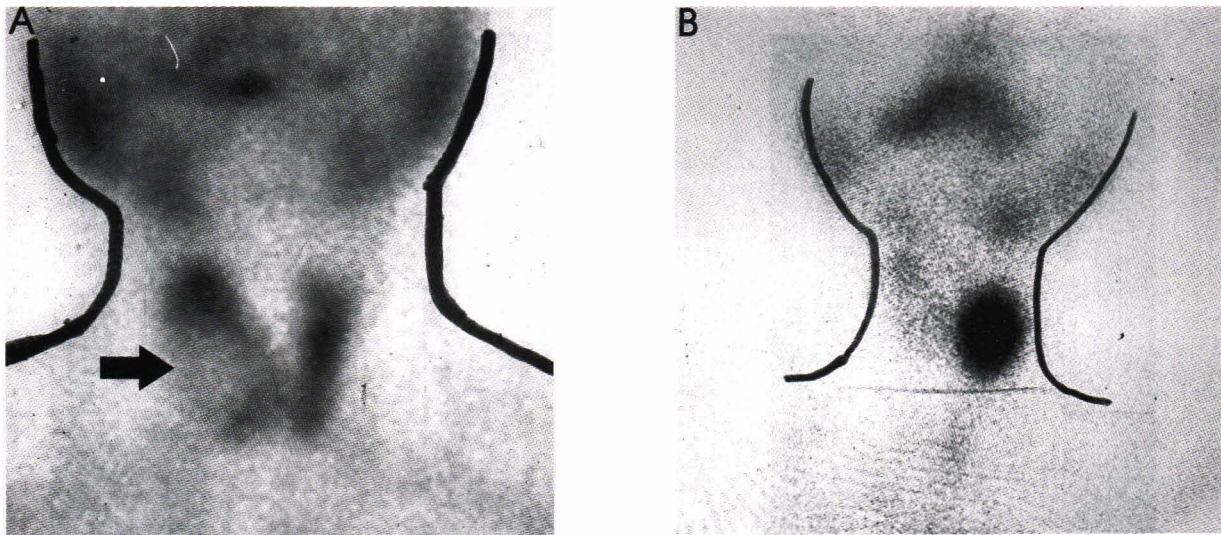


Figure 7. Thyroid scintigraphy

- A. Cold nodule of thyroid gland ; the study reveals an area of decreased radiotracer uptake occupying almost the area of right thyroid lobe.
- B. Toxic adenoma of thyroid gland ; the study reveals a single nodule with total suppression of the remainder of thyroid gland.

4. Parathyroid glands.

Parathyroid glands produce parathyroid hormone which has four main functions i.e., increase calcium absorption from gastrointestinal tract, stimulate osteoclastic cell moving calcium and phosphate from the bone, stop reabsorption of phosphate at proximal renal tubules resulted to phosphaturia and increase reabsorption of calcium at renal tubules resulted to hypercalcemia. Parathyroid tumor produces excessive parathyroid hormone leads to hypercalcemia, hypophosphatemia, bone disease, renal stones, peptic ulcer, pancreatitis or pseudogout.

Skeletal plain radiographs can suggest hyperparathyroidism such as subperiosteal resorption at radial aspect of phalangeal bones, abnormal vascular and periarticular ligamentous calcification or band-like demineralization and dense vertebral end-plates of the spine (Rugger-Jersey appearance) (Figure 8) or salt and pepper appearance of the cranial

vault, etc. Imaging of neck region will be performed only to serve the purpose of pre-operative localization. Scintigraphy or US or MRI sensitivity are comparable for localization.

There are two techniques of scintigraphy, $^{201}\text{Tl}/^{99\text{m}}\text{Tc}$ pertechnetate subtraction technique ($^{201}\text{Tl}/^{99\text{m}}\text{Tc}$ subtraction) and double-phase $^{99\text{m}}\text{Tc}$ -MIBI technique. The principle of the first technique is both normal thyroid tissue and parathyroid adenoma will capture ^{201}Tl while only thyroid gland capture $^{99\text{m}}\text{Tc}$. When the image of ^{201}Tl is subtracted by the $^{99\text{m}}\text{Tc}$ image, the radiopharmaceuticals will remain in the parathyroid adenoma if it exists, except the tumor is less than 3 mm in size.⁽⁸⁾ However false positive can be found in thyroid neoplasm, colloid goiter, focal Hashimoto's thyroiditis and least common in metastatic carcinoma, lymphoma and sarcoidosis.⁽⁹⁾ The more accurate technique is $^{99\text{m}}\text{Tc}$ -MIBI. $^{99\text{m}}\text{Tc}$ -MIBI (methoxyisobutyl isonitrile) is lipophilic cationic

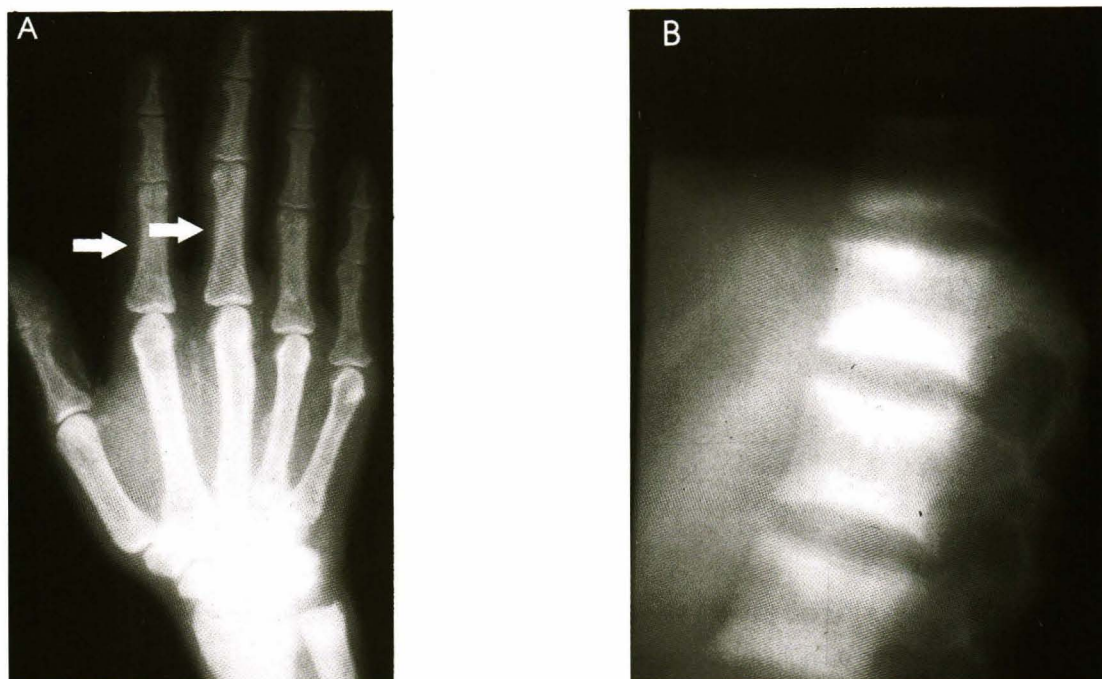


Figure 8. Skeletal plain radiograph of a patient with hyperparathyroidism.

- A. Plain radiograph of left hand shows subperiosteal resorption at radial aspect of proximal phalangeal bones (arrow) and abnormal calcified vessels.
- B. Plain radiograph of thoraco-lumbar spine shows dense vertebral end-plates.

: With courtesy of Dr. Boonyaporn Vasuratna

complex which will be captured by mitochondria. Organs which have more mitochondria will capture more radiopharmaceuticals. Imaging will be performed by SPECT in double phases. The early image will be performed at 15 minutes post radiopharmaceutical administration and the late image will be done at 2-3 hours later. Both thyroid gland and parathyroid adenoma will capture $^{99m}\text{Tc-MIBI}$ promptly in the early phase image but in the late image only parathyroid adenoma still shows hot spot (Figure 9). This technique shows 90 % sensitivity. ⁽¹⁰⁾

Ultrasonography or MRI is useful for treatment follow-up. MRI will detect mediastinal parathyroid adenoma which 85 % of the patients showed hyperSI on T2WI.

5. Adrenal glands.

Adrenal glands are paired endocrine glands located at suprarenal region. Right adrenal gland is more superior and lateral to the kidney than the left one which is posterior to splenic vessels at the level of pancreatic tail (Figure 10). The shape of adrenal gland may be changed according to the cross-sectional imaging level. The right adrenal shapes can be linear or inverted V or K configuration while the left one is linear, inverted V, triangular, inverted Y or star-like. The average width of each limb is 2-3 mm. but should be less than 5 mm. ⁽¹¹⁾ Most of the cortisol-producing adrenal masses are bigger than 2 cm. which can be clearly detected on CT or MRI. CT is the first choice in terms of clearly outlined by the

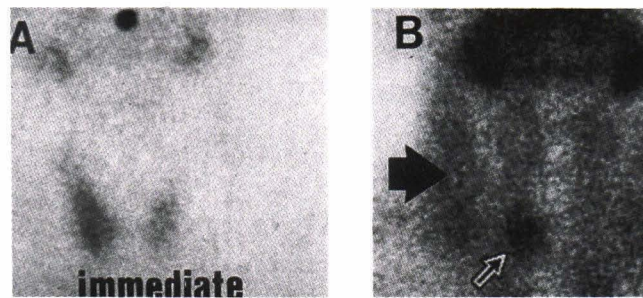


Figure 9. Double phase ^{99m}Tc-MIBI parathyroid scintigraphy.

- A. Immediate image shows prominent right thyroid lobe
- B. Late image shows obvious intense focus in right lower lobe of thyroid gland (small arrow). A large parathyroid adenoma near the right lower pole of thyroid gland was found at surgery. Note the significant activity in the strap muscles of the neck on the delayed images, a normal finding (large arrow).

Source : Mike M, Albert TL, Marc QC. Sestamibi Parathyroid Imaging. Semin Nucl Med 1995;25 (3): 221-34

excessive fat (Figure 11), shorter examination time and cheaper than MRI.

About 50 % of adrenal carcinomas will produce an endocrine disorder. Cushing syndrome is the commonest which may be seen alone or in combination with virilization. Functioning tumors are usually large when presenting and are readily detected by CT often seen as large, irregularly shaped heterogeneous masses in the adrenal region with some central areas of low attenuation because of necrosis.

Heterogeneous enhancement is typically seen. In the small adrenocortical carcinoma, it can be difficult to distinguish a well-differentiated carcinoma from an adenoma either by imaging or needle biopsy.⁽¹²⁾ With multiplanar capability and the high tissue contrast of T2 – weighted images, MRI can be useful to define the adrenal origin and the extent of the carcinoma for staging and therapeutic management.⁽¹³⁾

Pheochromocytoma arises from neural crest tissue (adrenal medulla). Ten percent of pheochro-

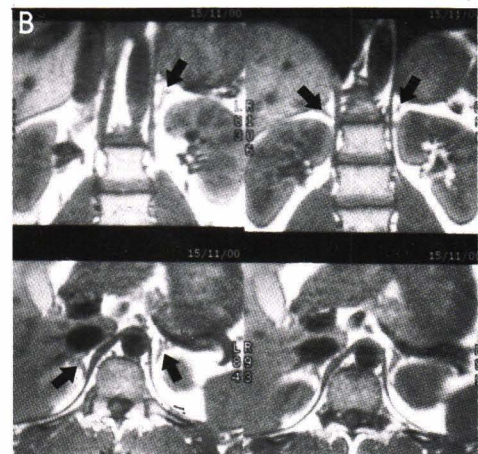
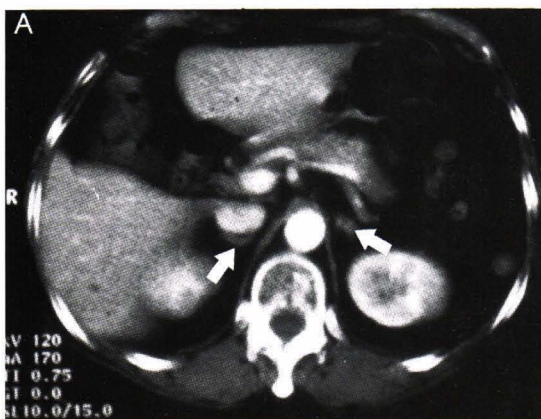


Figure 10. CT scan and MRI of normal adrenal glands

- A : CT scan of normal left and right adrenal glands (arrow)
- B : MRI (T1 WI) of normal left and right adrenal glands (arrow)



Figure 11. CT scan of a patient with Cushing's syndrome reveals adenoma at left limb of adrenal gland (2), meanwhile right adrenal gland is normal (arrow).
: With courtesy of Dr. Laddawan Vajragupta

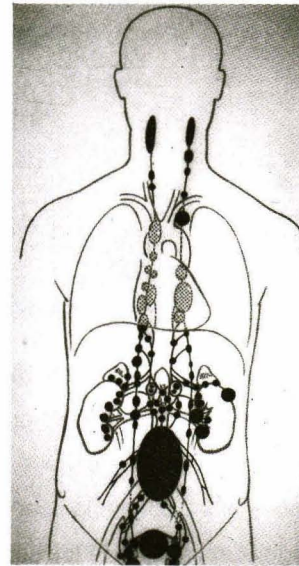


Figure 12. Possible location of pheochromocytoma
Source : Mangr WM, Gifford RW. Pheochromocytoma. New York, Springer-Verlag 1977

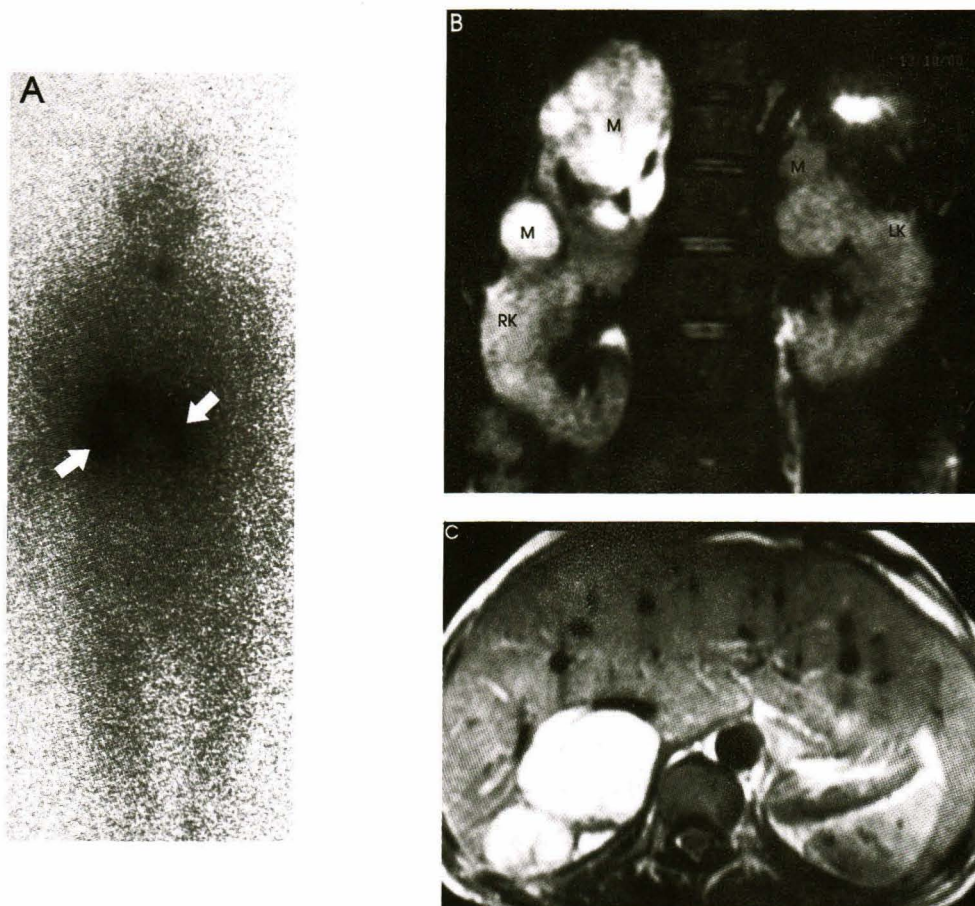


Figure 13. Pheochromocytoma

- A. ^{131}I -MIBG whole body scintigraphy shows radiotracer uptake of pheochromocytomas which locate at both adrenal glands. (arrow)
- B. Coronal view of MRI (T2 WI) with fat saturation reveals inhomogeneous intensity of a large lobulated right adrenal mass and small left adrenal mass (M).
- C. Contrast-enhanced sagittal MRI (T1 WI) reveals a large adrenal mass with very bright enhancement.

mocytoma can be bilateral, 15 % are in the extra-adrenal sympathetic paraganglia which mostly located in the abdomen above aortic bifurcation (organ of Zuckerkandl) (Figure 12). Imaging diagnosis can be done by CT, MRI or ¹³¹I-MIBG (Metaiodobenzylguanidine). Sensitivity of CT in detecting pheochromocytoma is 90 - 95 % comparable to MRI. MRI will show marked bright SI on T2WI because of large amount of fluid content and vascularity. Focal bright SI on T1WI representing bleeding spots may be found. ¹³¹I-MIBG shows sensitivity of 88 - 90% ⁽¹⁴⁾ and specificity of 98 - 100 %. ⁽¹⁵⁾ MIBG (guanethidine analog) is captured by chromaffin cells which are component of pheochromocytoma. Moreover, this technique shows extra-adrenal pheochromocytoma more effectively than other modalities (Figure 13).

6. Pancreas

Most common endocrine tumor in the pancreas is islet cell tumor which is usually small but can be demonstrated by CT (Figure 14. A) or MRI or late

capillary or venous phase of selective angiography which shows hypervascular homogenous staining ⁽¹⁶⁾ (Figure 14 B). In case of inconclusive imaging finding but clinically still suggested, splenic venous sampling or intra-operative US should be performed for accurate surgical planning. ⁽¹⁷⁾

References

1. Quint DJ. Hypothalamic, pituitary, and pineal Imaging. In: Sandler MP, Patton JA, Gross MD, Shapiro B, Falke THM, eds. Endocrine Imaging. Norwalk, Connecticut: Appleton & Lange, 1992:119 - 47
2. Mark L, Pech P, Daniels D, Charles C, Williams A, Haughton V. The pituitary fossa : a correlative anatomic and MR study. Radiology 1984 Nov; 153 (2): 453 - 7
3. Fujisawa I, Asato R, Kawata M, Sano Y, Nakao K, Yamada T, Imura H, Naito Y. Hyperintense signal of the posterior pituitary on T1-weighted MR images : an experimental study. J

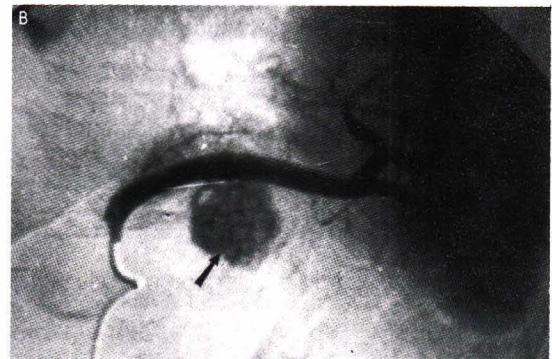


Figure 14. CT scan and splenic angiography of insulinoma

- A. CT scan shows a small enhancing mass (arrow) of pancreatic insulinoma at body of pancreas.
- B. Selective splenic arteriography (DSA) shows a homogeneous enhancing tumor mass.

- Comput Assist Tomogr 1989 May - Jun;13(3): 371 - 7
4. Simonetta AB. Imaging of suprasellar and parasellar tumors. Neuroimag Clin North Am 1999 Nov; 9(4): 717 - 32
 5. Yousem DM , Arrington JA, Zinreich SJ,Kumar AJ, Bryan RN. Pituitary adenoma : possible role of bromocriptine in intratumoral hemorrhage. Radiology 1989 Jan;170(1): 239 - 43
 6. Reiter RJ. The pineal gland. In: De Groot LJ,ed. Endocrinology Vol. 1. 2nd ed. Philadelphia: WB Saunders,1989. 240 - 53
 7. Sandler MP, Rao BK, Patton JA, Shaff MI, Powers TA. Thyroid imaging. In:Sandler MP, Patton JA, Gross MD, Shapiro B, Falke THM, eds. Endocrine Imaging. Norwalk, Connecticut: Appleton & Lange, 1992: 205 - 9
 8. Falk THM, Schipper J, Patton JA, Sandle MP. Parathyroid glands. In: Sandler MP, Patton JA, Gross MD, Shapiro B, Falke THM, eds. Endocrine Imaging. Norwalk Connecticut: Appleton & Lange, 1992: 159 - 61
 9. Metter FA,Guiberteau MJ. Parathyroid imaging. In: Metter FA,ed. Essentials of Nuclear Medicine Imaging,4th ed, Pennsylvania : W.B. Saunders, 1998: 125 - 7
 10. Taillefer R, Boucher Y, Potvin C, Lambert R. Detection and localization of parathyroid adenomas in patients with hyperparathyroidism using a single radionuclide imaging procedure with technitium-99m sestamibi. (double-phase study) J Nucl Med 1992 Oct; 33(10): 1801 - 7
 11. Gross MD, Falke THM, Shapiro B, Sandler MP. Adrenal glands. In : Sandler MP, Patton JA, Gross MD, Shapiro B, Falke THM, eds. Endocrine Imaging. Norwalk, Connecticut: Appleton & Lange,1992: 271 - 85
 12. Desai MB, Kapadia SN. Feminizing adrenocortical tumors in male patients : Adenoma versus carcinoma. J Urol 1988; 139: 101 - 3
 13. Kenney PJ, Lee JKT. The adrenals. In : Lee JKT, Sagel SS, Stanley RJ,Heiken JP. Computed body tomography with MRI correlation.4th ed, Lippincott-Raven Publishers, Philadelphia- New York 1998. 1171 - 1208
 14. Stark DD,William G,Bradler JR. Magnetic Resonance Imaging .2nd ed.St. Louis: Mosby-Year Book, 1992: 1801 - 4
 15. Mettler FA, Guiberteau MJ. Adrenal imaging. In: Metter FA, ed. Essentials of Nuclear Medicine Imaging,4th ed, Pennsylvania : W.B.Saunders, 1998: 365 - 7
 16. Troncone L. Radiolabelled metaiodobenzylguanine in the diagnosis of neural crest tumor. In: Murray IPC, Eil PJ, eds. Strauss HM. Nuclear Medicine in Clinical Diagnosis and Treatment. New York: Churchill Livingstone, 1994.745 - 56
 17. Francis TR, Quint LE, Falke THM, Cho KJ. Gastrointestinal endocrine tumor. In: Sandler MP, Patton JA, Gross MD, Shapiro B, Falke THM, eds. Endocrine Imaging. Norwalk, Connecticut: Appleton & Lange, 1992: 351 -75